Spectroscopic Determination of Magnetic Exchange Parameters and Structural Geometry for Trinuclear Compounds: $(CuL)_2Mn\cdot xB$ (L = *N*-(4-Methyl-6-oxo-3-azahept-4-enyl)oxamato and B = $(CH_3)_2SO$ ($x = 2$) or H_2O ($x = 5$))

Olivier Cador,[†] Corine Mathonière,*[,†] Olivier Kahn,*[,†] Jean-Pierre Costes,[‡] Marc Verelst,[§] and Pierre Lecante[§]

Laboratoire des Sciences Moléculaires, Institut de Chimie de la Matière Condensée de Bordeaux, CNRS UPR No 9048, avenue du Docteur Schweitzer, 33608 Pessac, France, Laboratoire de Chimie de Coordination, CNRS UPR No 8241, 205 route de Narbonne, 31077 Toulouse, France, and Centre d'Elaboration de Matériaux et d'Etudes Structurales, CNRS UPR No 8011, 29 rue Jeanne Marvig, 31055 Toulouse, France

Received September 24, 1998

The optical absorption spectroscopy for the trinuclear compounds $Mn(CuL)_2\cdot xB$ with L standing for *N*-(4-methyl-6-oxo-3-azahept-4-enyl)oxamato and B = $(CH_3)_2SO$ ($x = 2$) (**1**) or H_2O ($x = 5$) (**2**) has been investigated in the 4−300 K temperature range. The crystal structure of **1** was known; it consists of isolated and neutral trinuclear units in which the central Mn^{II} ion is linked to two CuL complex ligands and two $(CH_3)_2SO$ molecules in a cis configuration. The Cu−Mn−Cu linkage is bent with an angle of 127°. The spectra for **1** and **2** exhibit narrow and intense Mn^{II} spin-forbidden transitions in the 24000−28000 cm^{-1} range, activated by an exchange mechanism. The temperature dependences of the main feature corresponding to the $^6A_1 \rightarrow {}^4A_1$, $^4E(G)$ Mn^{II} transitions have been recorded. Using a model proposed first by Tanabe and co-workers and adapted to the CuMnCu topology, a theoretical expression for the temperature dependence of the intensity of the transition has been derived and compared to the experimental data. The parameters of this expression are the angle α ($2\alpha = 180° - $ CuMnCu) and the interaction parameter between the local ground states, J ($\mathbf{H} = -J\mathbf{S}_{Mn}\cdot(\mathbf{S}_{Cu1} + \mathbf{S}_{Cu2})$). For **1**, $\alpha = 26.5°$ was known from the structural data, and J has been found as -38 cm^{-1}. For **2**, J has been estimated as -32.6 cm^{-1} with $\alpha = 0°$. The spectra for **2** exhibit cold and hot bands; the energy difference between these bands depends on both J and the interaction parameter J^* between the Cu^{II} ions in their ground state and the Mn^{II} ion in its spin flip excited state. J^* has been estimated as $+35$ cm^{-1}. The linear geometry of the Cu−Mn−Cu linkage for **2** has been confirmed by a WAXS (wide-angle X-ray scattering) study. The intramolecular Cu···Cu distance has been estimated as 10.2 Å. These results have been discussed in relation to the information deduced from magnetic measurements.

Introduction

The field of molecular magnetic compounds has been increasingly attractive for two decades or so.[1] The control of the tridimensional assembleing of paramagnetic units in the crystal lattice (supramolecular architecture) to obtain a molecule-based magnet is still a challenge for the chemists working in this field. In other respects, the molecule-based magnets are often weakly colored, and an important issue is use of the light at the molecular scale for tuning the magnetic properties. Very recently, these ideas have been used to raise the long-range magnetic ordering temperature or reverse the magnetic poles by light irradiation of compounds belonging to the Prussian Blue family.[2,3]

Before studying the photomagnetic effects in molecule-based magnetic materials, it seemed to us that it was important to perform thorough studies of the optical properties of these species. Along this line, a few years ago we initiated a project concerning the absorption spectroscopy of magnetically coupled $Mn^{II}Cu^{II}$ compounds. Three papers have already been published. The first one deals with a $Mn^{II}Cu^{II}$ binuclear compound,[4] the second one deals with a linear $Mn^{II}Cu^{II}Mn^{II}$ trinuclear compound,[5] and the third one deals with a $Mn^{II}Cu^{II}_3$ tetranuclear species.[6] These three examples belong to the $Mn^{II}Cu^{II}$ compounds family synthesized and investigated in our research group.[7] They were selected to represent the elementary units found in polymeric systems as $Mn^{II}Cu^{II}$ chains[8] or $Mn^{II}_2Cu^{II}_3$ planar networks[9] showing a three-dimensional magnetic ordering at low temperature.

The spectra of the $Mn^{II}Cu^{II}$ compounds exhibit, in addition to a d−d transition due to the Cu^{II} ion, very narrow and intense

[†] Institut de Chimie de la Matière.
[‡] Laboratoire de Chimie de Coordination.
[§] Centre d'Elaboration de Matériaux et d'Etudes Structurales.

(1) Kahn, O. *Molecular Magnetism*; VCH : New York, 1993.
(2) Sato, O.; Iyoda, T.; Fujishima, K.; Hashimoto, K. *Science* **1996**, *272*, 704.
(3) Ohkoshi, S.; Yorozu, S.; Sato, O.; Iyoda, T.; Fujishima, A. *Appl. Phys. Lett.* **1997**, *70*, 1040.
(4) Mathonière, C.; Kahn, O.; Daran, J.-C.; Hilbig, H.; Köhler, F. H. *Inorg. Chem.* **1993**, *32*, 4057.
(5) Mathonière, C.; Kahn, O. *Inorg. Chem.* **1994**, *33*, 2103.
(6) Cador, O.; Mathonière, C.; Kahn, O. *Inorg. Chem.* **1997**, *36*, 1923.
(7) (a) Kahn, O. *Struct. Bonding (Berlin)* **1987**, *68*, 89. (b) Kahn, O. *Adv. Inorg. Chem.* **1995**, *43*, 179.
(8) Pei, Y.; Verdaguer, M.; Kahn, O.; Sletten, J.; Renard, J. P. *J. Am. Chem. Soc.* **1986**, *108*, 7428.
(9) Stumpf, H. O.; Pei, Y.; Kahn, O.; Sletten, J.; Renard, J. P. *J. Am. Chem. Soc.* **1993**, *115*, 6738.

10.1021/ic981147i CCC: $18.00
Published on Web 05/07/1999

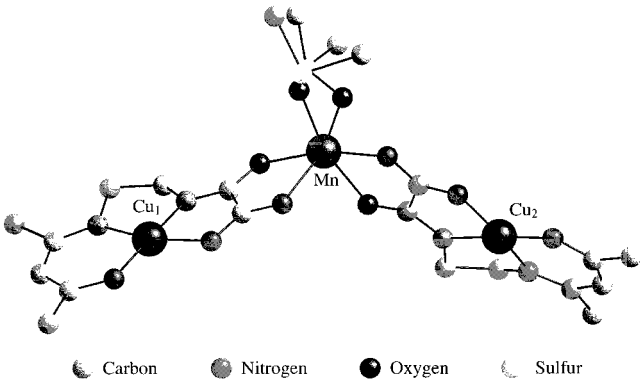

Figure 1. View of the compound **1**.

Mn^{II} formally spin-forbidden transitions. These transitions are activated by an exchange mechanism. Tanabe and co-workers proposed a model taking into account the interaction of incident light with a coupled pair of spins.[10] We adapted this model to the relevant molecular topologies. For the three compounds, it was shown that the interaction parameter J between the local ground states of Mn^{II} and Cu^{II} could be deduced from the analysis of the thermal dependence of the $^6A_1 \rightarrow {}^4A_1$, $^4E(G)$ Mn^{II} transitions. These J values were found to be in good agreement with those deduced from the magnetic data.

Recently, one of us reported on trinuclear compounds with the $Cu^{II}Mn^{II}Cu^{II}$ topology.[11] The formula of these compounds is $(CuL)_2Mn\cdot xB$ where L stands for the deprotonated form of *N*-(4-methyl-6-oxo-3-azahept-4-enyl)oxamic acid and B stands for a terminal ligand such as dimethyl sulfoxide (DMSO), water (H_2O), or pyridine. This paper is devoted to the optical absorption spectroscopy of two of these complexes: **1**, where B is DMSO ($x = 2$), and **2**, where B is H_2O ($x = 5$). The structure of **1** has already been determined by X-ray diffraction. It consists of isolated and neutral trinuclear units (Figure 1). In each unit, the central Mn^{II} ion is linked to two Cu^{II} ions through oxamato bridges. The copper atom is in a square planar environment, and the manganese atom completes an octahedral coordination with two DMSO molecules in a cis configuration. No single crystal of **2** suitable for X-ray diffraction and optical studies could be grown. In **2**, the CuMnCu linkage may be bent or linear, as previously described in refs 9 and 12 for similar Mn^{II} compounds with H_2O and DMSO ligands. The magnetic properties for **1** and **2** were also studied and revealed antiferromagnetic $Cu^{II}-Mn^{II}$ interactions. The interaction parameters J were found as -32.8 cm^{-1} for **1** and -33.8 cm^{-1} for **2**, using the spin Hamiltonian $\mathbf{H} = -J\mathbf{S}_{Mn}\cdot(\mathbf{S}_{Cu1} + \mathbf{S}_{Cu2})$.

Experimental Section

$Mn(CuL)_2\cdot 2DMSO$ (**1**) and $Mn(CuL)_2\cdot 5H_2O$ (**2**) were synthesized as microcristalline powders as described in reference 11.

Optical and Magnetic Measurements. The spectra were recorded with a CARY 5E spectrophotometer equipped with a continuous helium flow cryostat provided by Oxford Instruments and working down to 3.8 K. **1** and **2** were investigated in pellets prepared as follows: the powder samples were compacted with a cylinder press of 5 mm diameter under a 2 ton pressure during 90 min, stuck on a glass plate with cyanolite, and then polished to make them sufficiently transparent. For the low-temperature experiments, the plates were fixed in the cryostat with a silver paint. The band intensities were calculated from the area delimited by the absorption band and a linear baseline corresponding to the unique tangent to the spectra between two points situated on each side of the studied absorption band. These absorption intensities contain intrinsic errors due to the sloping background that are impossible to estimate accurately. At least two sets of data obtained from two different experiments and samples were used to determine the thermal dependence of absorption bands. The magnetic susceptibilities for **1** and **2** were measured with a Quantum Design MPMS-5S SQUID magnetometer at 1000 G in the 2−300 K temperature range.

WAXS Study. A powder sample of **2** was sealed in a Lindeman capillary. The spectrum scattered by the sample irradiated with graphite-monochromatized molybdenum Kα radiation ($\lambda = 0.71069$ Å) was obtained using a LASIP diffractometer.[13] In the range $0 < \theta < 65°$, 457 intensities corresponding to equidistant s points ($s = 4\pi(\sin q/l)$; $\Delta s = 0.035$ Å^{-1}) were collected. Measurements of air and Lindeman capillary scattering were performed in exactly the same conditions. The raw sample scattered intensity (sample + air + capillary) was corrected for air and capillary contributions by spectra subtraction, taking into account absorption from sample, and then corrected for polarization and self-absorption effects. Normalization was performed using Norman and Krogh-Moe's method.[14] The atomic scattering factors were taken from Cromer and Waber.[15] The reduced experimental radial distribution function (RDF) was calculated as indicated in ref 16. Theoretical structural models were built up using the CERIUS2 program.[17] The theoretical RDF was computed from the structural models by Fourier transform of the theoretical intensities calculated using the Debye formula.[18]

Results

The magnetic properties for **1** and **2** were measured on pellets prepared in a similar way as those used in optical spectroscopy. The $\chi_M T$ versus T curves, χ_M being the molar magnetic susceptibility and T the temperature, are similar to those given in ref 11. Therefore, the magnetic properties for **1** and **2** are not affected by the method used to prepare the samples. For our present purpose, it is important to note that the magnetic properties can be properly interpreted without introducing any temperature dependence of the interaction parameter J. Consequently, the structures for **1** and **2** were assumed not to vary significantly as a function of temperature.

The optical spectra at room temperature and 10 K for **1** are given in Figure 2. **2** presents similar spectra. Two regions can be distinguished: the copper region showing a very broad band centered at room temperature at 17950 cm^{-1} for **1** and 17850 cm^{-1} for **2** and the manganese region at higher energy showing a narrow band centered at room temperature at 24300 cm^{-1} and shoulders around 27 000 cm^{-1}. The broad band is attributed to Cu^{II} d−d electronic transitions. It corresponds to the $^2B_{1g} \rightarrow {}^2E_g$ transition of Cu^{II} in the idealized D_{4h} symmetry. As the temperature is lowered, the position of this band is not affected for **1**, while its width increases and its intensity decreases. Such

(10) (a) Ferguson, J.; Guggenheim, H. J.; Tanabe, Y. *J. Phys. Soc. Jpn.* **1966**, *21*, 692. (b) Ferguson, J.; Guggenheim, H. J.; Tanabe, Y. *J. Chem. Phys.* **1966**, *45*, 1134.
(11) Costes, J.-P.; Laurent, J.-P.; Moreno Sanchez, J. M.; Suarez Varela, J.; Ahlgren, M.; Sundgren, M. *Inorg. Chem.* **1997**, *36*, 4641.
(12) Stumpf, H. O.; Pei, Y.; Ouahab, L.; Le Berre, F.; Codjovi, E.; Kahn, O. *Inorg. Chem.* **1993**, 32, 5687.
(13) The LASIP diffractometer has a geometry specially set up for scattering measurements. It minimizes every external parasite scattering phenomenom.
(14) (a) Norman, N. *Acta Crytallogr.* **1957**, *10*, 370. (b) Krogh-Moe, J. *Acta Crytallogr.* **1956**, *9*, 951.
(15) Cromer, D.; Waber, T. *International Tables for X-ray Crystallography*; KYNOCH press: Birmingham, 1994.
(16) See, for example: (a) Mosset, A.; Lecante, P.; Galy, J. *Philos. Mag. B* **1982**, *46*, 137. (b) Burian, A.; Lecante, P.; Mosset A.; Galy, J. *J. Non-Cryst. Solids* **1987**, *90*, 633. (c) Laberty, C.; Verelst, M.; Lecante, P.; Mosset, A.; Alphonse, P.; Rousset, A. *J. Solid State Chem.* **1997**, *129*, 271. (d). Verelst, M.; Sommier, L.; Lecante, P.; Mosset, A.; Kahn, O. *Chem. Mater.* **1998**, *4*, 980.
(17) CERIUS2 molecular simulation program is supplied by BIOSYM technologies and runs on an Indy Silicon Graphics workstation.
(18) Debye, P. *Ann. Phys. (Leipzig)* **1915**, *46*, 809.

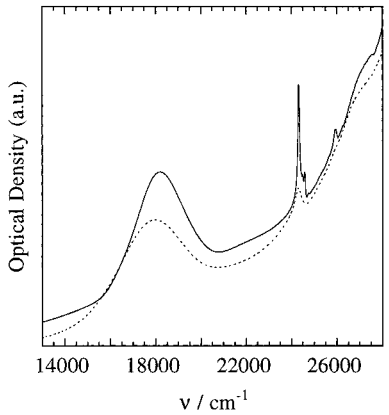

Figure 2. Absorption spectra for compound **1** at (- - -) room temperature and (—) 10 K in pellets.

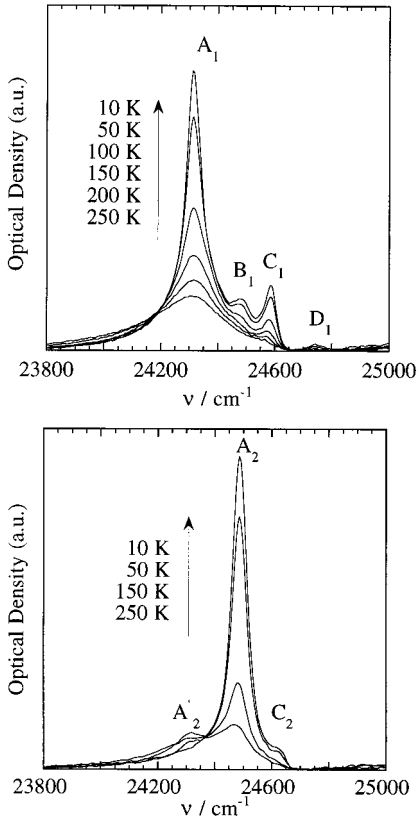

Figure 3. Absorption bands in the 23800−25000 cm^{-1} range for various temperatures: (top) compound **1**; (bottom) compound **2**.

a behavior is well documented and arises from vibronic coupling. The narrow band in the manganese region corresponds to the $^6A_{1g} \rightarrow {}^4A_{1g}$, $^4E_g(G)$ transitions of Mn^{II} in O_h local symmetry. These transitions correspond to a pure spin flip of an electron on the t_{2g} and e_g orbitals, and are not influenced by the ligand field at the first order. In contrast with the copper transition, the manganese transitions show a very pronounced enhancement of their intensity as the temperature is lowered along with the appearance of a multiplet. In Figure 3 the temperature dependences of the Mn^{II} transitions corrected for baseline for **1** and **2** are displayed. For **1**, four bands noted A_1, B_1, C_1, and D_1 are observed at low temperature; A_1 is located at 24310 cm^{-1}, B_1 at 24480 cm^{-1}, C_1 at 24585 cm^{-1}, and D_1 at 24745 cm^{-1}. For **2**, the Mn^{II} transitions are made up of three bands noted A_2', A_2, and C_2. They are located at 24319 cm^{-1} (band A_2'), 24486 cm^{-1} (band A_2), and 24624 cm^{-1} (band C_2). The A_1, B_1, C_1, and D_1 bands for **1** are cold bands; their intensities increase as the temperature is lowered. A_2 and C_2 are also cold bands, but A_2' is a hot band; its intensity decreases as the temperature is lowered. The bands A_i, $i = 1$ and 2, are tentatively assigned to the $^6A_1 \rightarrow {}^4A_1$ transitions, while the bands C_i are assigned to the $^6A_1 \rightarrow {}^4E$ transitions. This assignment is supported by the fact that the transition toward the $^4A_1$ state has always been found to be much more intense than the transition toward the ^4E state.[19] As **1** is prepared from a solution of **2**,[11] the band B_1 could be due to some traces of **2**. As a matter of fact, the intensity ratios between bands A_1 and B_1 are sample dependent. The energy of the band D_1 is 435 cm^{-1} higher than that of the band A_1. This energy gap exactly corresponds to the energy of the stretching vibration Mn−O(DMSO).[20] Therefore, the D_1 band is assigned to a vibronic assisted electronic transition. The origin of the band A_2' for **2** will be discussed in the following section.

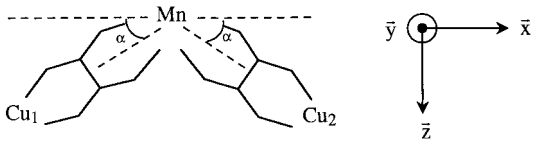

Figure 4. Schematic representation of compound **1** and reference axes adapted to the $MnCu_2$ topology.

Quantitative Interpretation of Optical Properties

Let us focus on the $^6A_1 \rightarrow {}^4A_1$, $^4E(G)$ transitions of Mn^{II}. In the following, we assume that all the intensity of the band comes from $^6A_1 \rightarrow {}^4A_1$. This assumption is justified by the fact that the bands C_i are 10 times as weak as the bands A_i.

The spin Hamiltonian describing the interaction between the metal ions may be written as

$$\mathbf{H} = -J\mathbf{S}_{Mn}\cdot\mathbf{S}_{Cu} \tag{1}$$

with

$$\mathbf{S}_{Cu} = \mathbf{S}_{Cu1} + \mathbf{S}_{Cu2} \tag{2}$$

where J is the interaction parameter, and $\mathbf{S}_{Mn}$, $\mathbf{S}_{Cu1}$, and $\mathbf{S}_{Cu2}$ are the local spins. In (1), all the anisotropy factors as well as the possible interaction between the terminal Cu^{II} ions are neglected. This Hamiltonian leads to four low-lying states $|\mathbf{S},\mathbf{S}_{Cu}\rangle$ with the following energies:

$$E(S,S_{Cu}) = -\frac{J}{2}(S(S+1) - S_{Cu}(S_{Cu}+1) - S_{Mn}(S_{Mn}+1)) \tag{3}$$

S, S_{Mn}, and S_{Cu} are the quantum numbers associated with the spins operators $\mathbf{S} = \mathbf{S}_{Mn} + \mathbf{S}_{Cu}$, $\mathbf{S}_{Mn}$, and $\mathbf{S}_{Cu}$, respectively. Let us call $\mathbf{S}^*_{Mn}$ the spin operator for the spin flip excited state of Mn^{II}. We assume that the magnetic interaction in this excited state can be written in the same form as in the ground state,

$$\mathbf{H}^* = -J^*\mathbf{S}^*_{Mn}\cdot\mathbf{S}_{Cu} \tag{4}$$

As in the ground state, this Hamiltonian leads to four energy levels written in the same ket basis as in the ground state. Let us now determine the symmetry labels of these levels. The idealized symmetry of the structurally characterized molecule **1** is C_2 with the two-fold axis along z, as defined in Figure 4. The coupling of the two Cu^{II} doublet states leads to $^1B + {}^3A$.

(19) Ferguson, J.; Güdel, H. U.; Krausz, E. R.; Guggenheim, H. J. *Mol. Phys.* **1974**, *28*, 879.
(20) Berney, C. V.; Weber, J. H. *Inorg. Chem.* **1968**, *7*, 283.

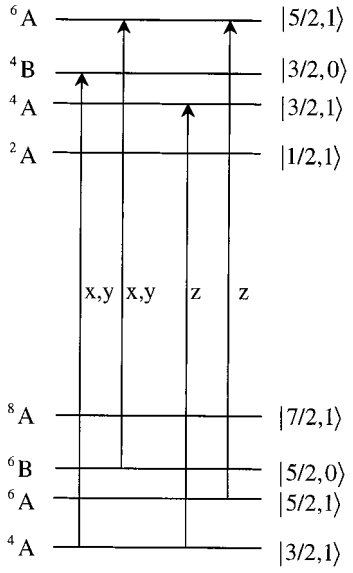

Figure 5. Relative energies and symmetry labels for the low-lying and excited states of compound **1** and optical subtransitions.

Coupling further with ^{6}A of Mn^{II} in C_2 symmetry results in A and B symmetry labels. The molecular states can then be written as ^{4}A, ^{6}A, ^{6}B, and ^{8}A in the ground state and ^{2}A, ^{4}A, ^{4}B, and ^{6}A in the excited state, where the superscripts refer to the total spin degeneracy of the molecule. Laporte and spin selection rules applied between ground and excited states give rise to four subtransitions whose polarizations are given in Figure 5.

We are now faced with the calculation of the relative intensities of the four subtransitions. As seen previously,[10] the Hamiltonian describing the interaction of the incident light and the molecule is given by

$$\mathbf{H}_E = \sum_{i,j} (\mathbf{\Pi}_{Mn_iCu_j} \cdot \mathbf{E})(\mathbf{s}_{Mn_i} \cdot \mathbf{s}_{Cu_j}) \tag{5}$$

where $\mathbf{s}_{Mn_i}$ is a monoelectronic spin operator referring to the ith 3d orbital of Mn^{II} and $\mathbf{s}_{Cu_j}$ is the spin operator referring to the singly occupied orbital on each Cu^{II}. **E** is the electric field of the incident light. The components of the vector $\mathbf{\Pi}_{Mn_iCu_j}$ are defined as

$$\Pi^t_{Mn_iCu_j} = \left(\frac{\partial J_{i,j}}{E^t}\right)_{E^t \to 0} \quad (t = x,y,z) \tag{6}$$

where $J_{i,j}$ is the interaction parameter between the ith 3d orbital of Mn^{II} and the magnetic orbital of the jth Cu^{II}. In the case of dipolar electric transitions, the transition moment vector **P** is defined as

$$\mathbf{P} = \sum_{i,j} \Pi_{Mn_iCu_j} (\mathbf{s}_{Mn_i} \cdot \mathbf{s}_{Cu_j}) \tag{7}$$

P acts only on the spin values. Then, the basis kets which have to be considered are in the form $|S, S_{Cu}, S_{Mn}\rangle$, both in the ground and excited states. The matrix elements of the transition moment between states $|S, S_{Cu}, S_{Mn}\rangle$ and $|S^*, S^*_{Cu}, S^*_{Mn}\rangle$ may be written as

$$\langle S,S_{Cu},S_{Mn}|\mathbf{P}|S^*,S^*_{Cu},S^*_{Mn}\rangle = \langle S,S_{Cu},S_{Mn}|\sum_{i,j} \Pi_{Mn_iCu_j} (\mathbf{s}_{Mn_i} \cdot \mathbf{s}_{Cu_j})|S^*,S^*_{Cu},S^*_{Mn}\rangle \tag{8}$$

Each subtransition $|S,S_{Cu}\rangle \rightarrow |S^*,S^*_{Cu}\rangle$ has a transition moment P written as $P(S,S_{Cu}; S^*,S^*_{Cu})$. The details of the calculation based on the irreducible tensor theory[21] and symmetry considerations are given as Supporting Information. Finally, the relative intensity is given as

$$I_{relat}(T) = \frac{\sum_{S,S_{Cu}} (2S+1) P^2(S,S_{Cu}; S^*,S^*_{Cu}) \exp\left(-\frac{E(S,S_{Cu})}{kT}\right)}{\sum_{S,S_{Cu}} (2S+1) \exp\left(-\frac{E(S,S_{Cu})}{kT}\right)} \tag{9}$$

or

$$I_{relat}(T) = \frac{A^2 \cos^2 \alpha \left(1 + \exp\left(\frac{7J}{2kT}\right)\right) + A^2 \sin^2 \alpha \left(\frac{3}{5} + \frac{7}{5} \exp\left(\frac{5J}{2kT}\right)\right)}{4 + 6 \exp\left(\frac{5J}{2kT}\right) + 6 \exp\left(\frac{7J}{2kT}\right) + 8 \exp\left(\frac{6J}{kT}\right)} \tag{10}$$

where A is a scaling factor and α the angle defined by $2\alpha = 180° - CuMnCu$ (see Figure 4). For **1**, $\alpha = 26.5°$ is given by the X-ray structure. Least-squares fitting of the experimental data leads to $J = -38$ cm^{-1}. For **2**, the α angle is not known. The two chemically relevant α values are 26.5° for the bent structure and 0° for the linear structure. J was then determined for these two α values and found as -27.4 cm^{-1} in the former case and -32.6 cm^{-1} in the latter. We will note that this latter solution is closer to that deduced from the magnetic data. We will see in the next section that the WAXS study confirms that the structure of **2** is linear. Theoretical and experimental curves are compared in Figure 6. For **2**, the theoretical curve obtained with $\alpha = 0°$ and $J = -32.6$ cm^{-1} is plotted. Let us now come back to the optical properties of **2**. The linear structure corresponds to $\alpha = 0°$. The theoretical spectrum is simplified and consists only of two transitions along the x axis: $|3/2,1\rangle \rightarrow |3/2,0\rangle$ and $|5/2,0\rangle \rightarrow |5/2,1\rangle$. Moreover, $|3/2,1\rangle \rightarrow |3/2,0\rangle$ is a cold band and $|5/2,0\rangle \rightarrow |5/2,1\rangle$ is a hot band. The band A_2 for **2** can then be assigned to the $|3/2,1\rangle \rightarrow |3/2,0\rangle$ transition and A_2' to the $|5/2,0\rangle \rightarrow |5/2,1\rangle$ transition. The energy gap between these two transitions is calculated as $(3J^*)/2 - (7J)/2$. A_2 and A_2' are separated by 167 cm^{-1}. Knowing the J value, -32.6 cm^{-1}, J^* is determined as $+35$ cm^{-1}.

WAXS Study

The spectroscopic data for **2** are compatible with two geometries, either a bent geometry as for **1** ($\alpha = 26.5°$) or a linear geometry ($\alpha = 0°$) with two H_2O molecules linked to Mn^{II} in a trans configuration. To obtain more insights on the structure of **2**, a WAXS study was performed. The WAXS technique allows the distance distributions for microcristalline powders to be determined. Bent and linear geometries are characterized by different Cu···Cu distances in the molecular unit, 9.78 Å for **1** and around 10.5 Å for a linear structure.

The first step was to build a structural model for **2**, assuming that the structure was bent as for **1**, then to determine the theoretical RDF arising from this model and to compare it with the experimental RDF for **2**. This comparison is shown in Figure 7a. The two RDF's are close to each other up to 5 Å but deviate significantly for higher distances. The bent geometry is certainly

(21) Weissbluth, M. *Atoms and molecules*; Academic Press: London, 1978

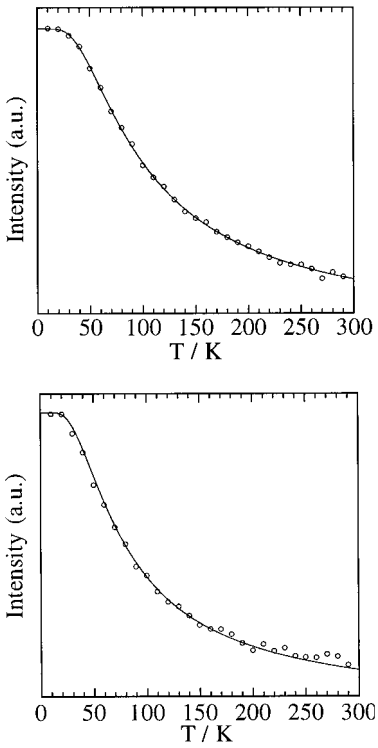

Figure 6. Temperature dependence of the absorption band $^6A_1 \rightarrow {}^4A_1$, ^4E: (○) experimental data; (—) calculated curve; (top) compound **1**; (bottom) compound **2**.

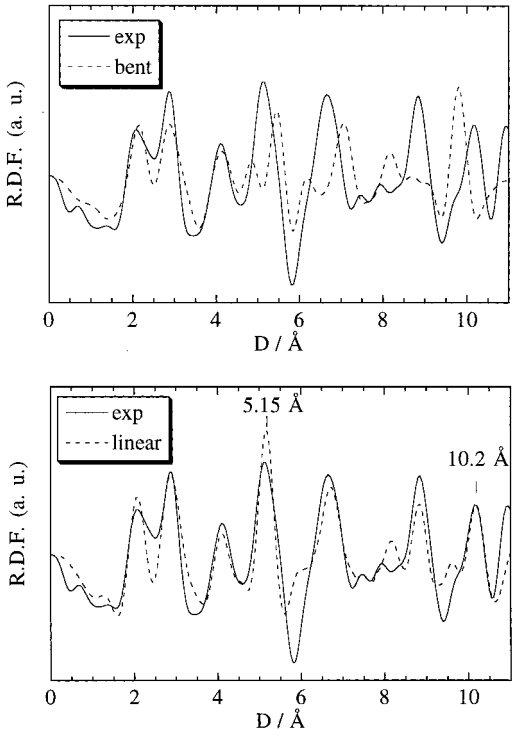

Figure 7. (—) Experimental radial distribution functions for compound **2** compared to (- - -) theoretical radial distribution functions calculated for the bent model (top) and the linear model (bottom).

not correct for **2**. The second step consisted of building a new structural model, assuming a linear geometry, and refining it. The RDF deduced from this new model is compared to the experimental one in Figure 7b. The theory−experiment agreement is now satisfying up to 12 Å. The best fit was obtained with the Cu···Mn distance fixed at 5.15 Å. The Cu···Cu distance is then found to be equal to 10.2 Å. The simulation procedure

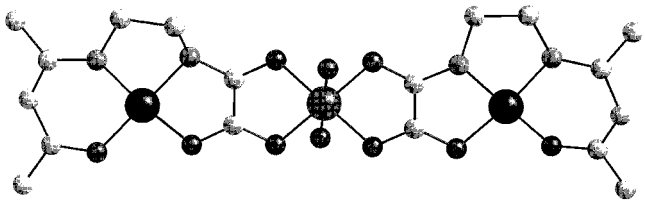

Figure 8. View of the plane molecular model proposed for compound **2**.

led to Cu···L(ligands) distances in the 1.90−1.95 Å range, and Mn···L distances around 2.15 Å. These distances are very close to those observed for **1**.

This WAXS study confirms the linear geometry for **2**. The structural model deduced from this study is represented in Figure 8. The Cu^{II} ion retains a square planar environment. The Mn^{II} ion has an octahedral environment, with two water molecules in a trans configuration.

Discussion

With this paper dealing with the optical absorption properties of $Mn^{II}Cu^{II}$ molecular compounds, all the possible topologies around the Mn^{II} ion have now been investigated: one bridge in the pair MnCu[4] and in the trinuclear compound MnCuMn,[5] two bridges in the trinuclear compound CuMnCu (this paper), and finally three bridges in the tetranuclear compound $MnCu_3$.[6]

The CuMnCu compound may be bent or linear, with the same bridging networks. In other respects, the values of the interaction parameters, *J*, are expected to be close to each other for the bent and linear compounds. As a matter of fact, the magnetic measurements could not distinguish the two geometries. The optical data depend on the CuMnCu angle, and their analysis shows that the two geometries lead to reasonable *J* values. The *J* values determined from optical data are probably less accurate than those deduced from magnetic measurements. Therefore, it is not possible to decide unambiguously whether the structure of **2** is bent or linear from the only optical data. However, the *J* value deduced from the optical data in the linear case is very close to that deduced from the magnetic data, which suggests that a linear structure is more likely. This structural prediction was confirmed by the WAXS technique.

The Mn^{II} spin-forbidden transitions are 3 times as narrow for **1** and **2** as for the previously investigated compounds. Although they are much broadened even at 10 K so that all the individual spin components (seen in Figure 5) cannot be resolved, several interesting features are visible at low temperature. In particular, the two transitions $^6A_1 \rightarrow {}^4A_1$ and $^6A_1 \rightarrow {}^4E$ appear at different energies, due to the lowering of symmetry around Mn^{II} with respect to O_h. The energy gap between these transitions is 275 cm^{-1} for **1** and 138 cm^{-1} for **2**. The difference between these two values may be attributed to the fact that the Mn^{II} environment is more distorted for **1** than for **2**.

Adapting the Tanabe formalism to the CuMnCu topology, the thermal dependences of the $^6A_1 \rightarrow {}^4A_1$ Mn^{II} transition were reproduced with $J = -38$ cm^{-1} for **1** and $J = -32.6$ cm^{-1} for **2**. These values are similar to those deduced from the magnetic measurements $J = -32.8$ cm^{-1} for **1** and $J = -33.8$ cm^{-1} for **2**. In the theoretical treatment, the contribution from the ^4E state was neglected. Taking into account this ^4E state would only change the values of the $\mathbf{\Pi}_{Mn_iCu_j}$ coefficients. The scaling factor *A* would be modified, but not the relative intensities. The intensity mechanism would remain entirely valid.

In the case of the linear compound **2**, the theoretical spectrum is composed of two transitions, A_2' and A_2 according to our

assignment, and J^* may be directly estimated from the energy gap between these two bands. J^* was found as $+35$ cm^{-1}. The situation is more complicated for the bent compound **1**. The spectrum is then composed of four transitions; two are associated with cold bands separated by J^* in energy, and two are associated with hot bands separated by J in energy. At low temperature, only the cold transitions are expected to be active, $|3/2,1\rangle \rightarrow |3/2,0\rangle$ and $|3/2,1\rangle \rightarrow |3/2,1\rangle$ with an intensity ratio of 1:5. Unfortunately, only the envelope of the two cold transitions is observed. At higher temperature, the four transitions contribute to the spectrum. A theoretical spectrum was simulated with $J = -38$ cm^{-1} and $J^* = +35$ cm^{-1}. This spectrum consists of two bands separated by 190 cm^{-1} at room temperature. These two bands should be resolved in the experimental spectrum. In fact, the bent and linear compounds exhibit similar spectra, assuming that the four transitions form two groups, one constituted of hot bands and the other one of cold bands. It is surprising not to observe hot bands for **1**. Perhaps, the approximations made to simulate the spectra (Gaussian shapes for the bands and bandwidths fixed at 100 cm^{-1}, irrespective of the temperature) are too important. Morevover, the experimental bands are often asymmetric (see, for instance, the low-energy side in Figure 3a). It follows that it is not possible to estimate accurately J^* for **1**.

The J^* value found for **2** is positive, which means that the interaction in the excited state is ferromagnetic. This result contrasts with what has been found for the MnCuMn and $MnCu_3$ compounds. Perhaps, the sign of J^* depends on the spin topology. Let us note that we recently studied similar trinuclear entities $Cu^{II}Mn^{II}Cu^{II}$ in Mn^{II}-doped oxamato-bridged $Mg^{II}Cu^{II}$ chain compounds.[22] The optical features of the $^6A_1 \rightarrow {}^4A_1$, ^4E Mn^{II} transitions are then much the same as those obtained for **2**. In particular, a hot band is clearly observed, as for **2**, and the spectrum can be interpreted with a positive J^* value. The observation of such a hot band is for sure not an artifact. Antiferromagnetic interactions in the ground state and ferromagnetic interactions in the excited state of $Mn^{II}Cu^{II}$ pairs have also been reported by Ferré[23] and Ferguson.[24] In ref 24, the authors explained this change of sign by taking into account charge transfer states. Theoretical calculations applied on CuMnCu compounds are in progress to obtain more insights on this problem.

A last question arising from this study is the difference observed in the spectra for **1** and **2**. It might be due to the differences of the Mn^{II} coordination spheres or to different excited-state patterns. Further studies on other compounds would be necessary to answer this question.

Conclusion

This paper is part of a thorough study on the optical properties of $Mn^{II}Cu^{II}$ molecular compounds. The Tanabe formalism has been used to interpret quantitatively the temperature dependence of the spin flip Mn^{II} transitions. Several structural topologies have been considered. In all the cases, the value of the interaction parameter between the Mn^{II} and Cu^{II} ions in their ground state, J, deduced from the optical data is in good agreement with the value deduced from magnetic susceptibility measurements. The optical data, except in the case of the pair MnCu, also allowed us to estimate the value of the interaction parameter between Cu^{II} in its ground state and Mn^{II} in its spin flip excited state. Such information cannot be provided by the magnetic measurements. For the spin topology considered in this paper, J^* was found to be positive (ferromagnetic), contrary to what we reported for the MnCuMn and $MnCu_3$ topologies. This change of sign is surprising, and we try to figure out the origin of this.

In this work, some hints concerning the molecular structure of compound **2** were deduced from the optical data and confirmed by the WAXS technique. This information concerning the linear structure of compound **2** could not be obtained from the magnetic data. As a matter of fact, the optical data depend on the CuMnCu angle, while the magnetic data do not. There is another important difference between the two techniques which warrants emphasis. The high-temperature limit of the magnetic susceptibility does not provide any information on the coupling scheme between the metal ions. The thermal motion dominates and hides the magnetic interaction. On the other hand, the optical spectra show spin-forbidden Mn^{II} transitions activated by the exchange mechanism, even at room temperature.

In our laboratory, we are primarily concerned by the design of new molecular materials and the thorough investigation of their physical properties. The molecular nature of compounds **1** and **2** has some drawbacks arising from the molecular complexity. In particular, the optical spectra are not fully resolved, which reduces somewhat the information content of the spectra. Some of the features predicted by the theory cannot be analyzed. In particular, we have not been able to grow single crystals large enough for polarized absorption spectra. In the field of optical properties of coupled systems, two approaches are possible. One consists of studying model compounds, for instance by doping ionic phases. The information content of the spectra may be very rich. In the meantime, the output in terms of molecular chemistry is limited. The other approach consists of designing new molecular compounds, to characterize them properly, and to go as far as possible in the investigation of their physical properties, even if the amount of information is limited by the molecular complexity. Our opinion is that both approaches deserve to be developed.

Supporting Information Available: The detail of the calculation of the relative intensities. This material is available free of charge via the Internet at http://pubs.acs.org.

IC981147I

(22) Cador, O.; Mathonière, C.; Kahn, O. Manuscript in preparation.
(23) Ferré, J.; Régis, M. *Solid State Commun.* **1978**, *26*, 225.
(24) Ferguson, J.; Guggenheim, H. J.; Krausz, E. R. *J. Phys. C: Solid State Phys.* **1971**, *4*, 1866.